

Effects of Couple-stress Resultants on Thermo-electro-mechanical Behavior of Vibrating Piezoelectric Micro-plates Resting on Orthotropic Foundation

K. Khorshidi*, M. Ghasemi, M. Karimi, M. Bahrami

Department of Mechanical Engineering, Arak University, Arak, Iran.

Article info

Article history:

Received 10 July 2019

Received in revised form

08 September 2019

Accepted 14 September 2019

Keywords:

Couple-stress theory

Analytical approach

Orthotropic foundation

Piezoelectric micro-plate

Abstract

This work aimed to study the thermo-electro vibration of a piezoelectric micro-plate resting on the orthotropic foundation. To catch the small-scale effects of the structure, couple-stress theory was employed. Motions of the structure were modelled based upon different shear deformation theories including exponential, trigonometric, hyperbolic, parabolic, and fifth-order shear deformation theories. These modified shear deformation theories are capable of considering transverse shear deformation effects and rotary inertia. Equation of motions are derived with Hamilton's principle and to solve these equations an analytical approach is applied. Besides, Effect of different boundary conditions including SSSS, CSSS, CSCS, CCSS and CCCC are investigated. The present results are validated with the previously published results. In the result section, the influences of various parameters such as increasing temperature, boundary conditions, foundation parameters, thickness ratio, aspect ratio, external voltage and length scale on the natural frequencies of the plate are illustrated in detail.

Nomenclature

a	Length of the plate	σ_{ij}	Normal stresses
b	Width of the plate	m_{ij}	Couple stress tensor
h	Thickness of the plate	χ_{ij}	Curvature tensor
E	Young's modulus	E_i	Electric field
ν	Poisson's ratio	D	Electric displacement
ρ	Mass density	G	Shear modulus
u	Displacement in the x direction	ℓ	Material length scale parameter
v	Displacement in the y direction	F	Axial force
w	Displacement in the z direction	K_{gx}	Shear foundation parameter
T	Kinetic energy of the plate	K_{gy}	Shear foundation parameter
U	Strain energy of the plate	K_w	Winkler constant
W	Work done by external forces	c_d	Damping constant
δ	Variation operator	θ	Angle of orthotropic function
ω	Natural frequency of the plate	V_0	External electric voltage
ε_{ij}	Normal strains	Φ	Electric potential

*Corresponding author: K. Khorshidi (Associate Professor)

E-mail address: k-khorshidi@araku.ac.ir

<http://dx.doi.org/10.22084/jrstan.2019.19583.1097>

ISSN: 2588-2597

1. Introduction

Because of the excellent properties of piezoelectric materials, the micro-plates that are made of these materials have been used in a wide variety of fields such as ultrasonic, piezoelectric transducers, transistors, and many devices. Piezoelectric materials due to their electromechanical coupling effect improve static and dynamic behaviour of structures; because when these materials are under mechanical loads, they can produce electrical fields and when they are in electrical fields, they can produce mechanical deformations. Based on the experimental observations, it is evident that the elastic properties of piezoelectric materials are size dependent. For this reason, studying these materials in nano-micro-scale is of crucial importance. There have been many researches about piezoelectric materials in recent years [1–4].

Both experimental and molecular dynamics simulation results have shown that the scale effect has a significant role in nano- microstructures. Because the experimental and molecular dynamics simulation is computationally expensive and time-consuming, one alternative is to utilize the available knowledge of classical continuum mechanics. The classical continuum theory cannot explain the scale effect. The scale effect is the phenomenon that the size of the structure's component is comparable to the size of its material constituent so that in micro-scale the stiffness and strength of materials are larger than those in the macro-scale. As the scale effect is ignored in conventional continuum theories, these theories need to be developed for microstructures. Many theories for nano-micro-scale structures have been proposed such as nonlocal elasticity theory [5–7], strain gradient theory [8], and couple-stress theory [9]. The essence of the nonlocal elasticity theory is that the stress field at the reference point in an elastic continuum depends not only on strain at that point but also on the strain at every other point in the domain. Recently, the free vibration analysis of functionally graded rectangular nano-plates are analysed by khorshidi et al. [10]. The nonlocal elasticity theory is used in their research. Liu et al. [11] studied the thermo-electro-mechanical free vibration of piezoelectric nano-plates using nonlocal theory. Li et al. [12] analysed buckling and free vibration of magneto-electro-elastic nano-plate resting on Pasternak foundation based on nonlocal theory. Fleck and Hutchinson [13] proposed strain gradient theory. In this theory, the second-order deformation tensor separated stretch gradient tensor and rotation gradient tensor. Ansari et al. [14] studied free vibration of functionally graded micro-beams based on strain gradient theory. Mindlin and Tiersten [15] proposed couple stress theory. According to this theory, the strain and curvature tensor are asymmetric. To consider the nonlocal effects in the governing equations, the material length scale parameters (MLSPs) must be taken into account. Classical

couple-stress theory besides the lame's constants, contains two additional material length scale parameters. In this theory, rotations depend on displacement. The modified couple stress theory that contains only one material length scale parameter proposed by Yang et al. [16]. Additionally, in this theory contrary to classical couple-stress theory strain and curvature tensor are symmetric. Lei et al. [17] carried out a size-dependent functionally graded micro-plate model using a modified couple stress theory requiring only one MLSP. The proposed model uses for both shear and normal deformation effects by a parabolic variation for all displacements across the thickness. Shojaefard et al. [18] investigated the free vibration and buckling of micro FG porous circular plate subjected to a nonlinear thermal load. The governing equations were derived using the modified couple-stress theory. Farzam and Hassani [19] analysed thermal and mechanical buckling of functionally graded carbon nanotube reinforced composite plates based on modified couple-stress theory. A refined hyperbolic shear deformation theory was used for buckling analysis, which satisfies free transverse shear stress conditions on the top and bottom surfaces of plate without a need for shear correction factor.

Classical Plate Theory (CPT) or Kirchhoff plate theory and First-order Shear Deformation Theory (FSDT) are well-known theories and are widely used for the analysis of nano-micro plates. CPT leads to accurate results for thin plates, while as the transverse shear deformation is neglected in this theory, when the thickness of the plates increases the accuracy of results decreases. In FSDT influence of rotary inertia and transverse shear deformation is considered. Moreover, in FSDT, the shear correction factor is required because the transverse shear deformation stresses are assumed to be constant across the thickness and cannot satisfy the free surface conditions. Additional modified theories have been proposed by many researchers [20–23] that in these theories the shear correction factor is not required. In recent years based on these theories, many articles have been established. Hosseini-Hashemi et al. [24] presented buckling of isotropic rectangular plates subjected to in-plane loaded. in their research An analytical closed-form solution was developed. In this solution method use of approximation for a combination of six different boundary conditions is not required. Hassani and Gholami [25] studied thermoelastic functionally graded (FG) rotating disks with nonuniform thickness under lateral pressure using numerical and analytical solutions. Thai and Choi [26] presented a simple FSDT to study the bending and free vibration of functionally graded plates. The theory presented in this research was built upon the classical plate theory. Khorshidi and Fallah [27] studied the buckling response of functionally graded nano-plate based on exponential shear deformation theory. The theory presented in this research was built upon the classical plate theory. Moreover, they investigated the

effect of exponential stress resultant on the buckling response of functionally graded rectangular plates based on exponential shear deformation theory [28]. Shi et al. [30] proposed a new Hyperbolic Tangent Shear Deformation theory (HTSDT) for the static, free vibration and buckling analysis of laminated composite plates. In the present theory, shear stresses disappear at the top and bottom surfaces of the plates and shear correction factors are no longer required. Tanzadeh and Amoushahi [31] developed a finite strip method for buckling and free vibration analysis of piezoelectric laminated composite plates based on various plate theories such as Zigzag, Re-fined plate and other higher order shear deformation theory by variation of transverse shear strains through plate thickness in the form of parabolic, sine, and exponential.

The simplest model to describe the interaction between the plate and foundation is the winkler model, which considers the foundation as a series of separated spring without coupling effect between each other. Pasternak [32] developed the Winkler model. Pasternak added a shear spring to show the influence of the interaction between the springs in Winkler model. Orthotropic Pasternak foundation [33] is another model to describe the interaction between the plate and foundation. In this model, normal, transverse, shear, and damping loads are considered while in Winkler's only normal loads are considered.

In this paper, vibrational behaviour of piezoelectric microplates resting on the orthotropic foundation subjected to thermal and electrical load was studied. The small-scale effects of the microplate were captured according to the couple stress theory. A single partial differential equation for transverse vibration of microplate was derived using a simple method, and analytical solution of vibrating microplate is presented for five different boundary conditions. In the result section, influences of different variables on frequencies are discussed.

2. Formulation

Yang et al. [16] proposed the modified couple-stress theory. They developed the classical couple-stress theory in which curvature and strain tensor are symmetric. Moreover, modified couple-stress theory contains only one MLSP that is another advantage of this theory over classical couple-stress theory. According to the modified couple-stress theory, curvature and strain tensor are defined as [11, 20].

$$\begin{aligned} \varepsilon_{ij} &= \frac{1}{2}(u_{i,j} + u_{j,i}) \\ \chi_{ij} &= \frac{1}{2}(\omega_{i,j} + \omega_{j,i}) \\ \omega_i &= \frac{1}{2}e_{ijk}u_{k,j} \\ E_i &= -\Phi_{,i} \end{aligned} \quad (1)$$

where u_i are displacement vectors and ω_i are rotation vectors. E_i are electric fields and ϕ is the electric potential. Constitutive relations are also given by [11, 20].

$$\begin{aligned} \sigma_{ij} &= C_{ijkl}\varepsilon_{kl} + e_{ijk}E_k - \lambda_{ij}\Delta T \\ D_i &= e_{ikl}\varepsilon_{kl} + \mu_{ik}E_k + p_i\Delta T \\ m_{ij} &= 2G\ell^2\chi_{ij} \end{aligned} \quad (2)$$

Here σ_{ij} and m_{ij} denotes the stress and couple stress tensor, respectively. e_{ijk} , C_{ijkl} and μ_{ik} are piezoelectric, elastic and dielectric coefficients, respectively. D_i denotes the electric displacement. G and ℓ are shear module and material length scale parameter, respectively and E_k are electric fields.

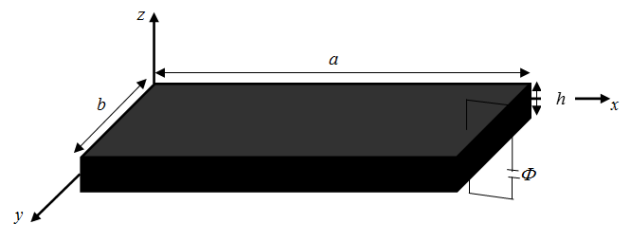


Fig. 1. Schematic of piezoelectric rectangular micro-plate.

3. Modified Shear Deformation Theories

Consider a piezoelectric rectangular micro-plate of length a , width b , and thickness h , as shown in Fig. 1. Modified shear deformation theories is employed to give the displacement vector. The displacement of the proposed micro-plate is:

$$\begin{aligned} u_1(x, y, z, t) &= u(x, y, t) - z \frac{\partial w(x, y, t)}{\partial x} \\ &\quad + f_i(z)\psi_x(x, y, t) \\ u_2(x, y, z, t) &= v(x, y, t) - z \frac{\partial w(x, y, t)}{\partial y} \\ &\quad + f_i(z)\psi_y(x, y, t) \\ u_3(x, y, z, t) &= w(x, y, t) \\ \Phi(x, y, z, t) &= -g(z)\varphi(x, y, t) + \frac{2zV_0}{h}e^{i\omega t} \end{aligned} \quad (3)$$

where u , v , and w represent displacements of an arbitrary point along x , y , and z axes; V_0 is the external electric voltage applied on the upper surface; φ is the electric potential on the mid-plane and ω is the frequency related to the external electric voltage. ψ_x and ψ_y are the rotation functions of the mid-plane in the x and y directions, respectively. Various distributions for $f(z)$ including Exponential Shear Deformation Theory (ESDT), Trigonometric Shear Deformation Theory (TSDT), Hyperbolic Shear Deformation theory (HSDT), Parabolic Shear Deformation Theory (PSDT) and Fifth-order Shear Deformation Theory (FOSDT) are presented in Table 1.

Table 1
Different shear deformation theories.

Type of theory	$f_i(z)$
ESDT [33]	$ze^{-2(\frac{z}{h})^2}$
TSDT [34]	$\frac{h}{\pi} \sin\left(\frac{\pi z}{h}\right)$
HSDT [35]	$h \sinh\left(\frac{z}{h}\right) - z \cosh\left(\frac{1}{2}\right)$
PSDT [38]	$z\left(\frac{5}{4} - \frac{5z^2}{3h^2}\right)$
FOSDT [38]	$z\left(\frac{1}{h} - \frac{2z^2}{h^3} + \frac{8z^4}{5h^5}\right)$

The displacement strain field with the linear assumption of von-Karman strain can be obtained as follows:

$$\begin{aligned}
 \varepsilon_{11} &= \frac{\partial u_1}{\partial x} = \frac{\partial u}{\partial x} - z \frac{\partial^2 w}{\partial x^2} + f(z) \frac{\partial \psi_x}{\partial x} \\
 \varepsilon_{22} &= \frac{\partial u_2}{\partial y} = \frac{\partial v}{\partial y} - z \frac{\partial^2 w}{\partial y^2} + f(z) \frac{\partial \psi_y}{\partial y} \\
 \varepsilon_{12} &= \frac{1}{2} \left(\frac{\partial u_1}{\partial y} + \frac{\partial u_2}{\partial x} \right) = \frac{\partial u}{\partial y} + \frac{\partial v}{\partial x} - 2z \frac{\partial^2 w}{\partial x \partial y} \\
 &\quad + f(z) \left(\frac{\partial \psi_x}{\partial y} + \frac{\partial \psi_y}{\partial x} \right) \\
 \varepsilon_{23} &= \frac{1}{2} \left(\frac{\partial u_2}{\partial z} + \frac{\partial u_3}{\partial y} \right) = g(z) \psi_y \\
 \varepsilon_{31} &= \frac{1}{2} \left(\frac{\partial u_3}{\partial x} + \frac{\partial u_1}{\partial z} \right) = g(z) \psi_x \\
 g(z) &= \frac{\partial f(z)}{\partial z}
 \end{aligned} \tag{4}$$

And the curvature components from Eq. (1) and electric fields will be as what follows:

$$\begin{aligned}
 \omega_1 &= \frac{1}{2}(e_{123}u_{3,2} + e_{132}u_{2,3}) = \frac{1}{2}(u_{3,2} - u_{1,3}) \\
 \omega_2 &= \frac{1}{2}(e_{213}u_{3,1} + e_{231}u_{1,3}) = \frac{1}{2}(-u_{3,1} + u_{1,3}) \\
 \omega_3 &= \frac{1}{2}(e_{312}u_{2,1} + e_{321}u_{1,2}) = (u_{2,1} - u_{1,2}) \\
 \chi_{11} &= \frac{1}{2}(\omega_{1,1} + \omega_{1,1}) = \frac{1}{2} \left(2 \frac{\partial^2 w}{\partial x \partial y} - g(z) \frac{\partial \psi_y}{\partial x} \right) \\
 \chi_{22} &= \frac{1}{2}(\omega_{2,2} + \omega_{2,2}) = \frac{1}{2} \left(-2 \frac{\partial^2 w}{\partial x \partial y} + g(z) \frac{\partial \psi_x}{\partial y} \right) \\
 \chi_{33} &= \frac{1}{2}(\omega_{3,3} + \omega_{3,3}) = \frac{1}{2} g(z) \left(-\frac{\partial \psi_x}{\partial y} + g(z) \frac{\partial \psi_y}{\partial x} \right) \\
 \chi_{12} &= \frac{1}{2}(\omega_{1,2} + \omega_{2,1}) \\
 &= \frac{1}{4} \left(-2 \frac{\partial^2 w}{\partial x^2} + 2 \frac{\partial^2 w}{\partial y^2} + g(z) \frac{\partial \psi_x}{\partial x} - g(z) \frac{\partial^2 \psi_y}{\partial y} \right) \\
 \chi_{23} &= \frac{1}{2}(\omega_{2,3} + \omega_{3,2})
 \end{aligned} \tag{5}$$

$$\begin{aligned}
 &= \frac{1}{4} \left(-\frac{\partial^2 u}{\partial y^2} + \frac{\partial^2 v}{\partial x \partial y} - f(z) \frac{\partial^2 \psi_x}{\partial y^2} + g'(z) \psi_x \right. \\
 &\quad \left. + f(z) \frac{\partial^2 \psi_y}{\partial x \partial y} \right) \\
 \chi_{31} &= \frac{1}{2}(\omega_{3,1} + \omega_{1,3}) \\
 &= \frac{1}{4} \left(-\frac{\partial^2 u}{\partial x \partial y} + \frac{\partial^2 v}{\partial x^2} - f(z) \frac{\partial^2 \psi_x}{\partial x \partial y} - g'(z) \psi_y \right. \\
 &\quad \left. + f(z) \frac{\partial^2 \psi_y}{\partial x^2} \right) \\
 E_1 &= -\Phi_{,1} = -\frac{\partial \Phi}{\partial x} = g(z) \frac{\partial \varphi}{\partial x} \\
 E_2 &= -\Phi_{,2} = -\frac{\partial \Phi}{\partial y} = g(z) \frac{\partial \varphi}{\partial y} \\
 E_3 &= -\Phi_{,z} = -\frac{\partial \Phi}{\partial y} = -\gamma^2 f(z) \varphi - \frac{2V_0}{h} e^{i\omega t}
 \end{aligned}$$

4. Orthotropic Pasternak Foundation

The Winkler foundation only considers normal loads while orthotropic Pasternak foundation considers normal, transverse, shear, and damping loads. Due to the orthotropic Pasternak foundation, a force was applied on the micro-plate that can be determined as [33]:

$$\begin{aligned}
 F &= -K_{gx} \left(\cos^2 \theta \frac{\partial^2}{\partial x^2} W(x, y, z, t) \right. \\
 &\quad \left. + \sin 2\theta \frac{\partial^2}{\partial y \partial x} W(x, y, z, t) \right. \\
 &\quad \left. + \sin^2 \theta \frac{\partial^2}{\partial y^2} W(x, y, z, t) \right) \\
 &\quad - K_{gy} \left(\sin^2 \theta \frac{\partial^2}{\partial x^2} W(x, y, z, t) \right. \\
 &\quad \left. - \sin 2\theta \frac{\partial^2}{\partial y \partial x} W(x, y, z, t) \right. \\
 &\quad \left. + \cos^2 \theta \frac{\partial^2}{\partial y^2} W(x, y, z, t) \right) \\
 &\quad + K_w W(x, y, z, t) - c_d \frac{\partial}{\partial t} W(x, y, z, t)
 \end{aligned} \tag{6}$$

where K_{gx} and K_{gy} are shear foundation parameters, K_w and c_d are Winkler constant and damping constant, respectively. θ is also the angel of orthotropic foundation.

5. Vibration of Piezoelectric Micro-plate

The Hamilton's principle was employed To governing the equations of motion. The Hamilton's principle is obtained as what follows:

$$\int_0^t (\delta T + \delta W_f - \delta U) dt = 0 \tag{7}$$

Strain energy, kinetic energy, and work done by external forces in the piezoelectric microplate can be obtained as follows:

$$\begin{aligned}
 U = & \frac{1}{2} \int_A \int_{-\frac{h}{2}}^{\frac{h}{2}} (\sigma_{11}\varepsilon_{11} + \sigma_{22}\varepsilon_{22} + 2\sigma_{12}\varepsilon_{12} + 2\sigma_{13}\varepsilon_{13} \\
 & + 2\sigma_{23}\varepsilon_{23}) dz dA \\
 & + \frac{1}{2} \int_A \int_{-\frac{h}{2}}^{\frac{h}{2}} (m_{11}\chi_{11} + m_{22}\chi_{22} + m_{33}\chi_{33} + 2m_{12} \\
 & + m_{22}\chi_{12} + 2m_{13}\chi_{13} + 2m_{23}\chi_{23}) \\
 & - \frac{1}{2} \int_A \int_{-\frac{h}{2}}^{\frac{h}{2}} (D_1E_1 + D_2E_2 + D_3E_3) dz dA \quad (8)
 \end{aligned}$$

$$T = \frac{1}{2} \int_A \int_{-\frac{h}{2}}^{\frac{h}{2}} \rho(\dot{u}_i\dot{u}_i) dV \quad (9)$$

$$T = \frac{1}{2} \int_A \int_{-\frac{h}{2}}^{\frac{h}{2}} \rho \left[\left(\frac{\partial u_1}{\partial t} \right)^2 + \left(\frac{\partial u_2}{\partial t} \right)^2 + \left(\frac{\partial u_3}{\partial t} \right)^2 \right] dV$$

$$\begin{aligned}
 W_f = & \frac{1}{2} \int_A \left(F_x \delta \left(\frac{\partial w}{\partial x} \right)^2 + F_y \delta \left(\frac{\partial w}{\partial y} \right)^2 \right) \\
 & + F \delta u_3 dA \quad (10)
 \end{aligned}$$

$$W_f = \frac{1}{2} \int_A \left(F_x \frac{\partial^2 w}{\partial x^2} + F_y \frac{\partial^2 w}{\partial y^2} \right) + F \times (w) dA$$

$$F_x = F_{Px} + F_{Tx} + F_{Ex}, \quad F_y = F_{Py} + F_{Ty} + F_{Ey}$$

where A is domain of mid-plane of micro-plate (at $z = 0$); (F_{Px}, F_{Py}) , (F_{Tx}, F_{Ty}) and (F_{Ex}, F_{Ey}) are normal forces created by axial force P , temperature rise ΔT and external electric voltage that are given as [37].

$$\begin{aligned}
 F_{Px} = F_{Py} = & P, \\
 F_{Tx} = F_{Ty} = & \tilde{\lambda}_{11} h \Delta T, \quad (11) \\
 F_{Ex} = F_{Ey} = & -2\tilde{e}_{31} V_0
 \end{aligned}$$

By substituting Eqs. (7-9) into Eq. (6) and integrating by parts following equations will be obtained:

$$L_1\xi + L_2\psi + L_3\phi = L_4w \quad (12a)$$

$$L_5\xi + L_6\psi + L_7\phi = L_8w \quad (12b)$$

$$L_9\xi + L_{10}\psi + L_{11}\phi = L_{12}w \quad (12c)$$

$$L_{13}\xi + L_{14}\psi + L_{15}\phi = L_{16}w \quad (12d)$$

where the operator L_i is defined by:

$$\begin{aligned}
 L_1 \equiv & (A_{17} + A_{18}) \frac{\partial^2}{\partial x \partial y} + \left(\frac{D_5}{4} \right) \left(\frac{\partial^4}{\partial x \partial y^3} + \frac{\partial^4}{\partial x^3 \partial y} \right) \\
 & - \left(\frac{D_8}{2} + \frac{3D_6}{4} \right) \frac{\partial^2}{\partial x \partial y}
 \end{aligned}$$

$$L_6 \equiv (A_{17} + A_{18}) \frac{\partial^2}{\partial x \partial y} + \left(\frac{D_5}{4} \right) \left(\frac{\partial^4}{\partial x \partial y^3} + \frac{\partial^4}{\partial x^3 \partial y} \right)$$

$$- \frac{D_8}{4} \frac{\partial^2}{\partial x \partial y} - \frac{D_6}{2} \frac{\partial^2}{\partial x^2} - \frac{D_6}{4} \frac{\partial^2}{\partial x \partial y}$$

$$L_2 \equiv A_{16} \frac{\partial^2}{\partial y^2} + A_{18} \frac{\partial^2}{\partial x^2} - A_{19}$$

$$+ \left(\frac{D_5}{4} \right) \left(\frac{\partial^4}{\partial x^2 \partial y^2} + \frac{\partial^4}{\partial x^4} \right)$$

$$+ \left(\frac{D_8}{2} + D_6 \right) \frac{\partial^2}{\partial x^2} + \left(\frac{D_6}{4} \right) \frac{\partial^2}{\partial y^2}$$

$$- \frac{D_7}{4} - I_6 \frac{\partial^2}{\partial t^2}$$

$$L_3 = L_{10} \equiv (B_5 + B_7) \frac{\partial}{\partial y}$$

$$L_4 \equiv (A_{13} + 2A_{15}) \frac{\partial^3}{\partial x^2 \partial y} + A_{11} \frac{\partial^3}{\partial y^3}$$

$$- D_3 \frac{\partial^3}{\partial x^2 \partial y} - D_3 \frac{\partial^3}{\partial y^3} - I_5 \frac{\partial^3}{\partial y \partial t^2}$$

$$L_{14} \equiv (A_{13} + 2A_{15}) \frac{\partial^3}{\partial x^2 \partial y} + A_{11} \frac{\partial^3}{\partial y^3}$$

$$- \frac{3D_3}{2} \frac{\partial^3}{\partial x^2 \partial y} + \frac{D_3}{2} \frac{\partial^3}{\partial y^3}$$

$$L_5 \equiv A_{16} \frac{\partial^2}{\partial x^2} + A_{18} \frac{\partial^2}{\partial y^2} - A_{19} \quad (13)$$

$$- \left(\frac{D_5}{4} \right) \left(\frac{\partial^4}{\partial y^4} + \frac{\partial^4}{\partial x^2 \partial y^2} \right)$$

$$+ \left(\frac{D_8}{2} + \frac{D_6}{4} \right) \frac{\partial^2}{\partial y^2} + \left(\frac{3D_6}{4} \right) \frac{\partial^2}{\partial x^2}$$

$$- \frac{D_8}{4} \frac{\partial^2}{\partial x \partial y} - \frac{D_7}{4} - I_6 \frac{\partial^2}{\partial t^2}$$

$$L_7 = L_9 \equiv (B_5 + B_7) \frac{\partial \phi}{\partial x}$$

$$L_8 \equiv A_{11} \frac{\partial^3}{\partial x^3} + (A_{13} + 2A_{15}) \frac{\partial^3}{\partial y^2 \partial x}$$

$$- \frac{D_3}{2} \left(\frac{\partial^3}{\partial x^3} \right) - I_5 \frac{\partial^3}{\partial x \partial t^2}$$

$$L_{13} \equiv A_{11} \frac{\partial^3}{\partial x^3} + (A_{13} + 2A_{15}) \frac{\partial^3}{\partial y^2 \partial x}$$

$$+ \frac{D_3}{2} \frac{\partial^3}{\partial x \partial y^2} + \frac{D_3}{2} \frac{\partial^3}{\partial x^3} - I_5 \frac{\partial^3}{\partial x \partial t^2}$$

$$L_{11} = B_8 \nabla^2 - B_9$$

$$L_{12} = L_{15} \equiv B_3 \nabla^2$$

$$L_{16} \equiv A_{10} \frac{\partial^4}{\partial x^4} + (2A_{12} + 4A_{14}) \frac{\partial^4}{\partial x^2 \partial y^2} + A_{10} \frac{\partial^4}{\partial y^4}$$

$$\begin{aligned}
 & - \left(I_3 \frac{\partial^4}{\partial x^2 \partial t^2} + I_3 \frac{\partial^4}{\partial y^2 \partial t^2} \right. \\
 & \left. - F_x \frac{\partial^2}{\partial x^2} - F_y \frac{\partial^2}{\partial y^2} \right)
 \end{aligned}$$

moreover, A_i and B_i are given as:

$$\begin{aligned}
 \{A_{10}, A_{12}, A_{14}\} &= \int_{-\frac{h}{2}}^{\frac{h}{2}} \{\tilde{c}_{11}, \tilde{c}_{12}, \tilde{c}_{66}\} z^2 dz \\
 \{A_{11}, A_{13}, A_{15}\} &= \int_{-\frac{h}{2}}^{\frac{h}{2}} \{\tilde{c}_{11}, \tilde{c}_{12}, \tilde{c}_{66}\} z f(z) dz \\
 \{A_{16}, A_{17}, A_{18}\} &= \int_{-\frac{h}{2}}^{\frac{h}{2}} \{\tilde{c}_{11}, \tilde{c}_{12}, \tilde{c}_{66}\} f(z)^2 dz \\
 A_{19} &= \int_{-\frac{h}{2}}^{\frac{h}{2}} \tilde{c}_{44} \left(\frac{\partial f(z)}{\partial z} \right)^2 dz \\
 \{I_3, I_5, I_6\} &= \int_{-\frac{h}{2}}^{\frac{h}{2}} \rho \{z^2, z f(z), f(z)^2\} dz \\
 \{B_3, B_5\} &= \int_{-\frac{h}{2}}^{\frac{h}{2}} \{z, f(z)\} \tilde{e}_{31} \gamma \sin(\gamma z) dz \\
 B_8 &= \int_{-\frac{h}{2}}^{\frac{h}{2}} \tilde{\kappa}_{11} \cos^2(\gamma z) dz \\
 B_9 &= \int_{-\frac{h}{2}}^{\frac{h}{2}} \tilde{\kappa}_{33} (\gamma \sin(\gamma z))^2 dz \\
 B_7 &= \int_{-\frac{h}{2}}^{\frac{h}{2}} \tilde{e}_{15} \frac{\partial f(z)}{\partial z} \cos(\gamma z) dz \\
 \{D_1, D_2, D_3, D_4, D_5, D_6, D_7, D_8\} &= \\
 & \int_{-\frac{h}{2}}^{\frac{h}{2}} \{10, f(z), f'(z), f''(z), f^2(z), (f'(z))^2, \\
 & (f''(z))^2, f(z)f'(z)\} C_{44} \ell^2 dz
 \end{aligned} \tag{14}$$

Now ϕ , ψ and ξ can be obtained in terms of w according to elimination method in solving systems of linear equations from Eqs. (12a), (12b), and (12c).

$$\Gamma_1 \zeta = \Gamma_2 w, \quad \Gamma_1 \psi = \Gamma_3 w, \quad \Gamma_1 \phi = \Gamma_4 w \tag{15}$$

where the operator Γ_i is given as:

$$\begin{aligned}
 \Gamma_1 &= L_{11}L_2L_5 - L_{10}L_3L_5 - L_1L_{11}L_6 \\
 & \quad + L_1L_{10}L_7 + L_3L_6L_9 - L_2L_7L_9 \\
 \Gamma_2 &= L_{12}L_3L_6 - L_{11}L_4L_6 - L_{12}L_2L_7 \\
 & \quad + L_{10}L_4L_7 + L_{11}L_2L_8 - L_{10}L_3L_8 \\
 \Gamma_3 &= -L_{12}L_3L_5 + L_{11}L_4L_5 + L_1L_{12}L_7 \\
 & \quad - L_1L_{11}L_8 - L_4L_7L_9 + L_3L_8L_9 \\
 \Gamma_4 &= L_{12}L_2L_5 - L_{10}L_4L_5 - L_1L_{12}L_6 \\
 & \quad + L_1L_{10}L_8 + L_4L_6L_9 - L_2L_8L_9
 \end{aligned} \tag{16}$$

Finally, taking operator Γ_1 from both sides of Eq. (12d) and using (15), transverse displacement equation of piezoelectric micro-plate can be obtained as follows:

$$L_{13}\Gamma_2 w + L_{14}\Gamma_3 w + L_{15}\Gamma_4 w = L_{16}\Gamma_1 w \tag{17}$$

6. Exact Solution

In this section, the natural frequency of piezoelectric micro-plates is obtained using a new simple analytical solution [37]. In this method, rotations are expressed in terms of transverse displacement and are substitute in transverse equation. This analytical solution for Eq. (16) can be used for different boundary conditions according Table 2. The solution that satisfies appropriate boundary conditions can be written in following form.

7. Numerical Results

To validate this model, results were compared with corresponding ones in open literature, then numerical results for vibration analysis of piezoelectric micro-plate under different boundary conditions including, SSSS, CSSS, CSCS, CCSS, CCCC are illustrated. Material properties of PZT4, which was used in this study, are given in Table 3.

Table 4 presents a comparison between the present study with those reported by Ke et al. [37] for first three dimensionless frequencies of SSSS, CCSS, and CCCC rectangular micro-plate. The material of micro-plate is assumed to be PZT4 and $\Delta T = 0$. Ke et al. investigated thermo-electro-mechanical vibration of the rectangular piezoelectric nano-plate based on the Mindlin plate theory under various boundary conditions. Table 4 also provides a comparison of the dimensionless frequencies $\bar{\omega} = \omega \frac{a^2}{h} \sqrt{\frac{\rho}{E}}$ for piezoelectric rectangular plate with those obtained by Bahreman et al. [39]. It is assumed that $E = 1.44\text{GPa}$, $\nu = 0.38$, $h = 88\mu\text{m}$, $\rho = 1220\text{kg/m}^3$. In this table, the effects of MLSP are shown. From Tables 3 and 4 it is evident that the excellent agreement between the present results and those reported by Ke et al. [37] confirms the high accuracy of the current analytical approach. According to Table 5, there is a bit difference between the results, which are obtained from various shear deformation theories. These differences are due to the fact that function $f(z)$ has different expansions through the thickness in various theories.

The dimensionless natural frequency of the rectangular micro-plate to study the influences of variation of length scale parameter are illustrated in Fig. 2 for SSSS boundary condition. In Fig. 2a, the dimensionless natural frequency of the rectangular micro-plate for various aspect ratios (a/b) are plotted and length to thickness ratio (a/h) is assumed to be $a/h = 10$.

Table 2
Admissible functions for various boundary conditions.

	Boundary conditions		Functions $X(x)$ and $Y(y)$	
	At $x = 0, x = L_1$	At $y = 0, x = L_2$	$X_m(x)$	$Y_n(y)$
SSSS	$X_m(0) = X_m''(0) = 0$ $X_m(L_1) = X_m''(L_1) = 0$	$Y_n(0) = Y_n''(0) = 0$ $Y_n(L_2) = Y_n''(L_2) = 0$	$\sin\left(\frac{m\pi x}{L_1}\right)$	$\sin\left(\frac{n\pi y}{L_2}\right)$
CSSS	$X_m(0) = X_m'(0) = 0$ $X_m(L_1) = X_m''(L_1) = 0$	$Y_n(0) = Y_n''(0) = 0$ $Y_n(L_2) = Y_n''(L_2) = 0$	$\sin\left(\frac{m\pi x}{L_1}\right) \left(\cos\left(\frac{m\pi x}{L_1}\right) - 1\right)$	$\sin\left(\frac{n\pi y}{L_2}\right)$
CSCS	$X_m(0) = X_m'(0) = 0$ $X_m(L_1) = X_m''(L_1) = 0$	$Y_n(0) = Y_n'(0) = 0$ $Y_n(L_2) = Y_n''(L_2) = 0$	$\sin\left(\frac{m\pi x}{L_1}\right) \left(\cos\left(\frac{m\pi x}{L_1}\right) - 1\right)$	$\sin\left(\frac{n\pi y}{L_2}\right) \left(\cos\left(\frac{n\pi y}{L_2}\right) - 1\right)$
CCSS	$X_m(0) = X_m'(0) = 0$ $X_m(L_1) = X_m'(L_1) = 0$	$Y_n(0) = Y_n''(0) = 0$ $Y_n(L_2) = Y_n''(L_2) = 0$	$\sin^2\left(\frac{m\pi x}{L_1}\right)$	$\sin\left(\frac{n\pi y}{L_2}\right)$
CCCC	$X_m(0) = X_m''(0) = 0$ $X_m(L_1) = X_m'(L_1) = 0$	$Y_n(0) = Y_n''(0) = 0$ $Y_n(L_2) = Y_n'(L_2) = 0$	$\sin^2\left(\frac{m\pi x}{L_1}\right)$	$\sin^2\left(\frac{n\pi y}{L_2}\right)$

Table 3
Material properties of PZT4.

Property	Value	Property	Value	Property	Value	Property	Value
E_0	1×10^9	c_{11}	$132E_0$	c_{44}	$26E_0$	e_{15}	10.5
E_1	1×10^9	c_{12}	$71E_0$	c_{66}	$30.5E_0$	e_{33}	14.1
E_2	1×10^5	c_{13}	$73E_0$	ρ	7500	h	$5E_1$
E_3	1×10^{-4}	c_{33}	$115E_0$	e_{31}	-4.1	κ_{11}	$5.841E_1$
κ_{33}	$7.124E_1$	λ_{11}	$4.738E_2$	λ_{33}	$4.529E_2$	$p_1 = p_3$	$0.25E_1$

Table 4
Comparison study of the first three dimensionless frequencies of SSSS, CCSS and CCCC piezoelectric rectangular micro-plate.

Boundary condition	Model	ω_1	ω_2	ω_3
SSSS	Present (ESDT)	0.5463	1.0143	1.5620
	Present (TSDT)	0.5462	1.0142	1.5619
	Present (HSDT)	0.5461	1.0141	1.5617
	Present (PSDT)	0.5461	1.0141	1.5617
	Present (FOSDT)	0.5641	1.0144	1.5619
	Ref. [37]	0.5453	1.0132	1.5594
	Present (ESDT)	0.7192	1.1854	1.7881
CCSS	Present (TSDT)	0.7191	1.1853	1.7880
	Present (HSDT)	0.7190	1.1851	1.7880
	Present (PSDT)	0.7190	1.1851	1.7880
	Present (FOSDT)	0.7190	1.1854	1.7883
	Ref. [37]	0.7184	1.1838	1.7868
CCCC	Present (ESDT)	0.9146	1.3691	2.0143
	Present (TSDT)	0.9142	1.3690	2.0141
	Present (HSDT)	0.9141	1.3689	2.0140
	Present (PSDT)	0.9141	1.3689	2.0140
	Present (FOSDT)	0.9142	1.3692	2.0143
	Ref. [37]	0.9137	1.3672	2.0096

Table 5
Comparison study of frequency parameters $\bar{\omega}$ for rectangular plate with those obtained by Bahreman et al. [39].

a/h	Model	ℓ/h					
		0	0.2	0.4	0.6	0.8	1
5	Present (ESDT)	5.2845	5.7747	7.0415	8.7514	10.6929	12.7607
	Present (TSDT)	5.2822	5.7711	7.0352	8.7421	10.681	12.7463
	Present (HSDT)	5.2813	5.7698	7.0330	8.7389	10.6766	12.7408
	Present (PSDT)	5.2813	7.7698	7.0330	8.7389	10.6766	12.7408
	Present (FOSDT)	5.2854	5.7764	7.0446	8.7559	10.6987	12.7678
	Ref. [39]	5.4165	5.9039	7.1695	8.8861	10.8414	12.9273
20	Present (ESDT)	5.9201	6.4030	7.6714	9.4125	11.4120	13.5560
	Present (TSDT)	5.9199	6.4027	7.6709	9.4118	11.4111	13.5548
	Present (HSDT)	5.9198	6.4027	7.6707	9.4116	11.4108	13.5545
	Present (PSDT)	5.9198	6.4027	7.6707	9.4116	11.4108	13.5548
	Present (FOSDT)	5.9201	6.4032	7.6716	9.4129	11.4125	13.5566
	Ref. [39]	5.9332	6.4158	7.6840	9.4257	11.4266	13.5723
100	Present (ESDT)	6.9711	6.4535	7.7217	9.4651	11.4689	13.6188
	Present (TSDT)	6.9711	6.4535	7.7217	9.4650	11.4689	13.6186
	Present (HSDT)	6.9711	6.4535	7.7217	9.4650	11.4689	13.6186
	Present (PSDT)	6.9711	6.4535	7.7217	9.4650	11.4689	13.6186
	Present (FOSDT)	6.9712	6.4535	7.7217	9.4651	11.4689	13.6187
	Ref. [39]	5.9717	6.4540	7.7229	9.4656	11.4695	13.6193

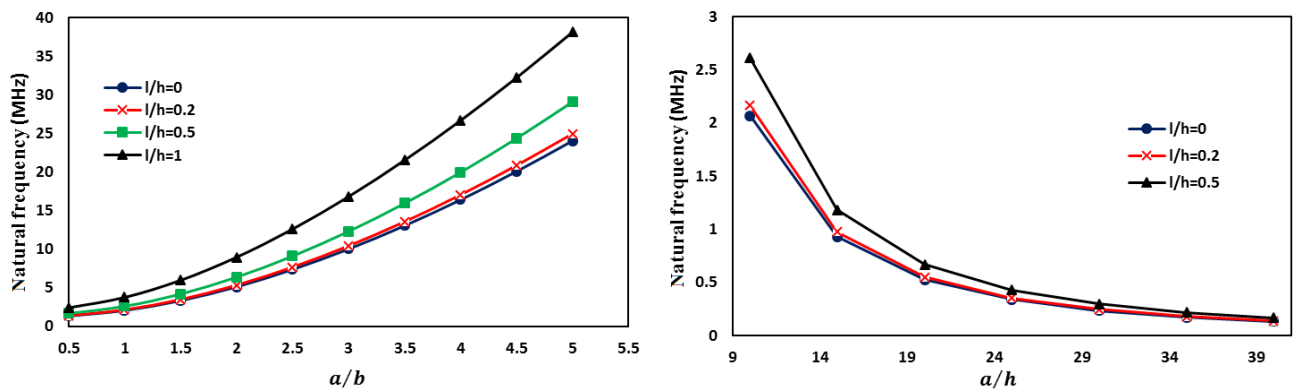


Fig. 2. Natural frequency of the rectangular micro-plate for SSSS boundary condition versus various, a) Aspect ratio (a/b), and b) Various length to thickness ratio (a/h).

Moreover, in Fig. 2b the dimensionless natural frequency of the rectangular micro-plate for various length to thickness ratios (a/h) are tabulated and aspect ratio (a/b) is assumed to be $a/b = 1$ also in Fig. 2, V_0 is considered to be zero. It is evident that the natural frequency of the micro-plate increases with increasing length scale parameter to thickness ratio (l/h); because with increasing the length scale parameter, the micro-plate becomes stiffer. Furthermore, the frequency raises by increasing aspect ratio because for a plate with length a , when the width of the plate decreases it leads into decreasing the degree of freedom, therefore the stiffness of plate and frequency will increase.

In Fig. 3, the effects of the temperature on the

dimensionless frequency of the piezoelectric rectangular micro-plate are shown. According to this figure, it seems that with increasing temperature, the dimensionless frequency decreases because by raising the temperature the stiffness of micro-plate decreases.

Figs. 4 and 5 depict the effects of orthotropic foundation on the vibration behavior of piezoelectric rectangular micro-plate. The dimensionless frequency versus K_{gx} for piezoelectric microplate is investigated in Fig. 4. Moreover, in this figure the effects of Winkler constant (K_w) are shown. It is obvious that increasing K_{gx} and K_w lead into increasing the dimensionless frequency of the piezoelectric rectangular micro-plate. The effects of the boundary conditions on the natural frequency of micro-plate are plotted in Fig. 5. It

is evident that when degrees of freedom of microplate decrease, the natural frequency increases because with decreasing degree of freedom, the micro-plate becomes stiffer.

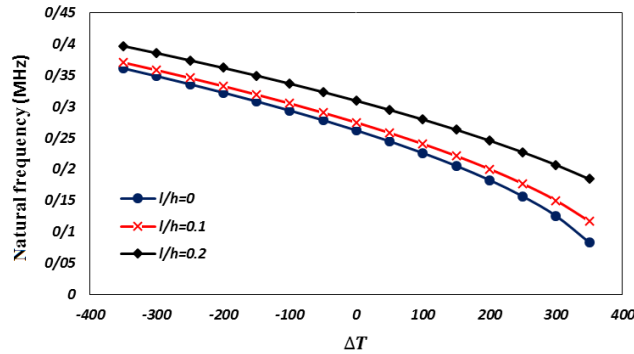


Fig. 3. The effects of the temperature on the dimensionless frequency of the SSSS piezoelectric rectangular micro-plate; $a/b = 1$, $a/h = 20$, $V_0 = 200V$.

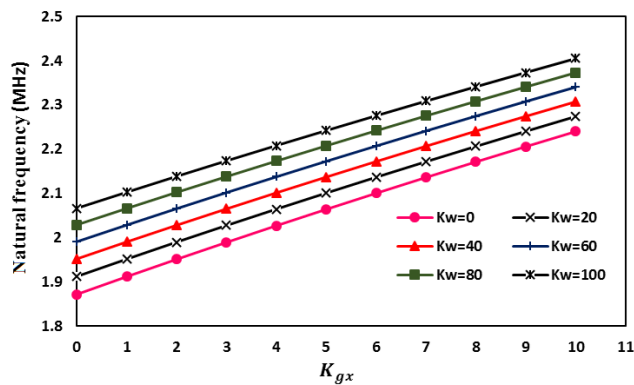


Fig. 4. The effects of the orthotropic Pasternak foundation on the dimensionless frequency of the SSSS piezoelectric rectangular micro-plate.

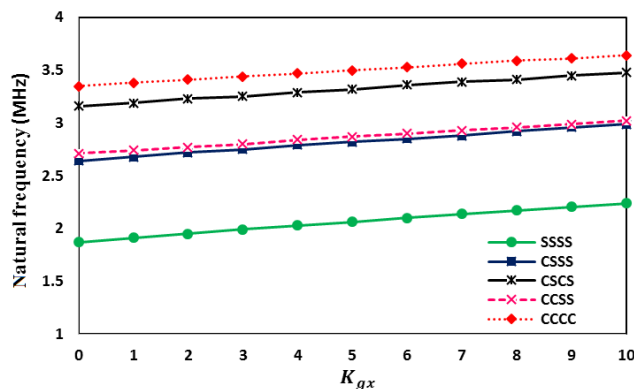


Fig. 5. The effects of the orthotropic Pasternak foundation and various boundary conditions on the dimensionless frequency of the piezoelectric rectangular micro-plate.

Furthermore, Fig. 6 demonstrates the effects of the orthotropic Pasternak foundation on the dimensionless frequency of the piezoelectric rectangular micro-plate

for various boundary conditions. It is seen that the dimensionless frequency increases by increasing Pasternak foundation parameters such as K_w and K_{gx} . It is also evident that the stability of the micro-plate increases when both K_{gx} and K_w increase. Moreover, it seems that the effect of the K_{gx} is more than K_w .

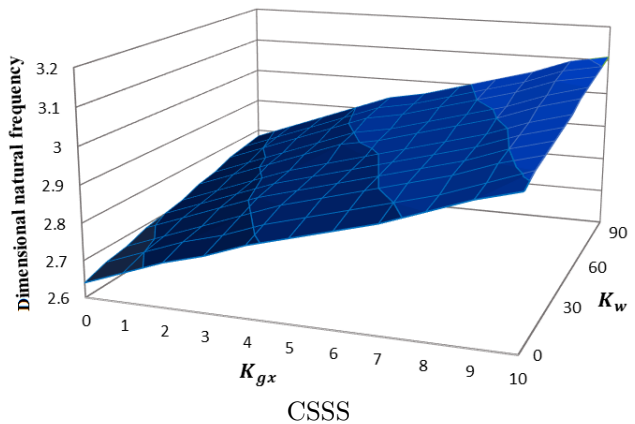
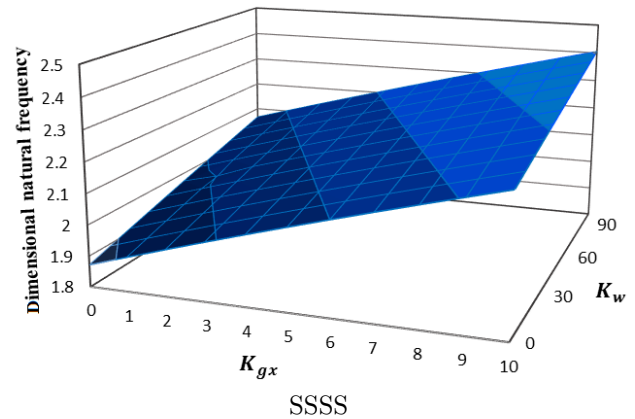


Fig. 6. The effects Winkler constant (K_w) and K_{gx} on the dimensionless frequency of the piezoelectric rectangular micro-plate corresponding to different boundary conditions.

In Figs. 7 and 8, the dimensionless frequency versus the orthotropic angle is investigated. These figures can be used to have a better understanding of the effect of the orthotropic foundation on the dimensionless frequency of micro-plate. If $K_{gy} > K_{gx}$, by increasing the orthotropic angle the dimensionless frequency raises until it reaches a maximum value. Then increase of the orthotropic angle leads into reducing the dimensionless frequency, while for $K_{gx} > K_{gy}$, this variations is inverse. It means that when $K_{gx} > K_{gy}$, increasing the orthotropic angle leads into reducing dimensionless frequency and this value reaches a minimum value. After that when the orthotropic angle increases the dimensionless frequency increases. Furthermore, the frequency raises by increasing aspect ratio because for a plate with length a , when the width of the plate decreases, it leads into decreasing the degree of freedom, therefore the stiffness of plate and frequency increase.

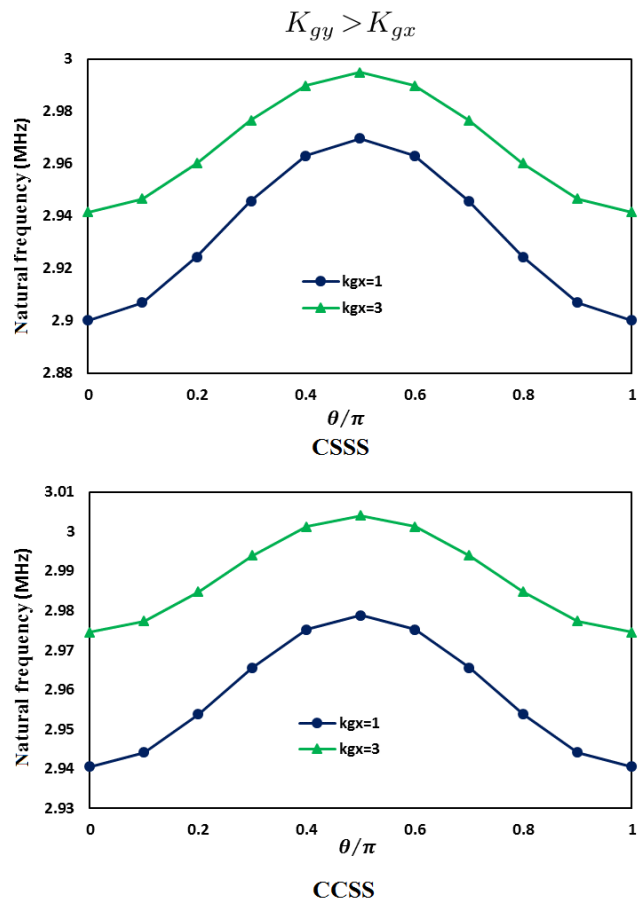
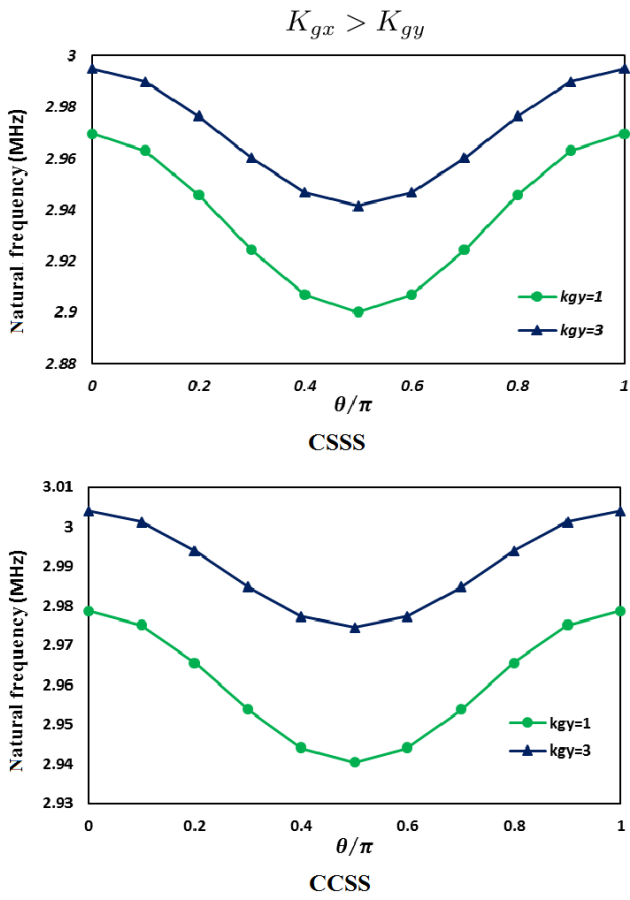


Fig. 7. The effects of the angel of orthotropic foundation and various boundary conditions on the dimensionless frequency of the rectangular micro-plate; $a/h = 10$, $a/b = 1$, $l/h = 0.2$, $K_w = 5$, $K_{gx} = 10$.

Fig. 8. The effects of the angel of orthotropic foundation and various boundary conditions on the dimensionless frequency of the rectangular micro-plate; $a/h = 10$, $a/b = 1$, $l/h = 0.2$, $K_w = 5$, $K_{gy} = 10$.

8. Conclusions

The present study contains thermo-electro vibration of piezoelectric micro-plate resting on the orthotropic foundation subjected to different boundary conditions. The formulations were based on the different shear deformation theories using the couple-stress theory, and Hamilton’s principle was used to drive the equations of motion.

The effect of different parameters such as thickness ratio, aspect ratio, increasing temperature, boundary conditions, foundation parameters, external voltage, and length scale on the natural frequencies of the plate was also studied. It was shown that,

- The natural frequency of micro-plate increases with increasing length scale parameter to thickness ratio (l/h), because with increasing the length scale parameter the micro-plate becomes stiffer.

- The natural frequency of micro-plate increases with increasing length scale parameter to thickness ratio (l/h), because with increasing the length scale parameter the micro-plate becomes stiffer.
- The dimensionless frequency increases by increasing Pasternak foundation parameters such as K_w and K_{gx} . Additionally, the stability of the micro-plate increases when both K_{gx} and K_w increase. Moreover, the effect of the K_{gx} is greater than K_w .
- With increasing temperature, the dimensionless frequency decreases because by raising the temperature the stiffness of micro-plate decreases.
- As boundary conditions get stronger support, rigidity of structure rises and frequency of vibration increases. Thus, frequency parameter is at the lowest in SSSS and is at the highest in CCCC.

References

- [1] C.K. Lee, Theory of laminated piezoelectric plates for the design of distributed sensors/actuators, Part I: Governing equations and reciprocal relationships, *J. Acoust. Soc. Am.*, 87(3) (1990) 1144-1158.
- [2] P.J.C. Branco, J.A. Dente, On the electromechanics of a piezoelectric transducer using a bimorph cantilever undergoing asymmetric sensing and actuation, *Smart Mater. Struct.*, 13(4) (2004) 631-642.
- [3] W.M. Zhang, G. Meng, D.I. Chen, Stability, Nonlinearity and reliability of electrostatically actuated MEMS devices, *Sensors*, 7(5) (2007) 760-796.
- [4] J.M. Dietl, A.M. Wickenheiser, E. Garcia, A Timoshenko beam model for cantilevered piezoelectric energy harvesters, *Smart Mater. Struct.*, 19(5) (2010) 055018.
- [5] A.C. Eringen, D.G.B. Edelen, On nonlocal elasticity, *Int. J. Eng. Sci.*, 10(3) (1972) 233-248.
- [6] A.C. Eringen, On differential equations of nonlocal elasticity and solutions of screw dislocation and surface waves, *J. Appl. Phys.*, 54(9) (1983) 4703-4710.
- [7] A.C. Eringen, *Nonlocal Continuum Field Theories*, Springer-Verlog New York Publisher, (2002).
- [8] E.C. Aifantis, Strain gradient interpretation of size effects, *Int. J. Fract.*, 95 (1/4) (1999) 299-314.
- [9] R.A. Toupin, Elastic materials with couple-stresses, *Arch. Rational Mech. Anal.*, 11(1) (1962) 385-414.
- [10] K. Khorshidi, T. Asgari, A. Fallah, Free vibrations analysis of functionally graded rectangular nanoplates based on nonlocal exponential shear deformation theory, *Mech. Advanced Compos. Struct.*, 2(2) (2015) 79-93.
- [11] C. Liu, L.L. Ke, Y.S. Wang, J. Yang, S. Kitipornchai, Thermo-electro-mechanical vibration of piezoelectric nanoplates based on the nonlocal theory, *Compos. Struct.*, 106 (2013) 167-174.
- [12] Y.S. Li, Z.Y. Cai, S.Y. Shi, Buckling and free vibration of magneto-electroelastic nanoplate based on nonlocal theory, *Compos. Struct.*, 111 (2014) 522-529.
- [13] N.A. Fleck, J.W. Hutchinson, A phenomenological theory for strain gradient effects in plasticity, *J. Mech. Phys. Solids*, 41(12) (1993) 1825-1857.
- [14] R. Ansari, R. Gholami, S. Sahmani, Free vibration analysis of size-dependent functionally graded microbeams based on the strain gradient Timoshenko beam theory, *Compos. Struct.*, 94(1) (2011) 221-228.
- [15] R.D. Mindlin, H.F. Tiersten, Effects of couple-stresses in linear elasticity, *Arch. Rational Mech. Anal.*, 11(1) (1962) 415-448.
- [16] F. Yang, A.C.M. Chong, D.C.C. Lam, P. Tong, Couple stress based strain gradient theory for elasticity, *Int. J. Solids Struct.*, 39(10) (2002) 2731-2743.
- [17] J. Lei, Y. He, B. Zhang, D. Liu, L. Shen, S. Guo, A size-dependent FG micro-plate model incorporating higher-order shear and normal deformation effects based on a modified couple stress theory, *Int. J. Mech. Sci.*, 104 (2015) 8-23.
- [18] M.H. Shojaeefard, H.S. Googarchin, M. Ghadiri, M. Mahinzare, Micro temperature-dependent FG porous plate: free vibration and thermal buckling analysis using modified couple stress theory with CPT and FSDT, *Appl. Math. Modell.*, 50 (2017) 633-655.
- [19] A. Farzam, B. Hassani, Thermal and mechanical buckling analysis of FG carbon nanotube reinforced composite plates using modified couple stress theory and isogeometric approach, *Compos. Struct.*, 206 (2018) 774-790.
- [20] J. Kim, K.K. Żur, J.N. Reddy, Bending, free vibration, and buckling of modified couples stress-based functionally graded porous micro-plates, *Compos. Struct.*, 209 (2019) 879-888.
- [21] M. Aydogdu, Comparison of various shear deformation theories for bending, buckling, and vibration of rectangular symmetric cross-ply plate with simply supported edges, *J. Compos. Mater.*, 40(23) (2006) 2143-2155.
- [22] K.P. Soldatos, A transverse shear deformation theory for homogeneous monoclinic plates, *Acta Mech.*, 94(3-4) (1992) 195-220.
- [23] V. Panc, *Theories of Elastic Plates*, Springer Netherlands, (1975).
- [24] S. Hosseini-Hashemi, K. Khorshidi, M. Amabili, Exact solution for linear buckling of rectangular Mindlin plates, *J. Sound Vib.*, 315(1-2) (2008) 318-342.
- [25] A. Hassani, M. Gholami, Analytical and numerical bending solutions for thermoelastic functionally graded rotating disks with nonuniform thickness based on mindlin's theory, *J. Stress Anal.*, 2(1) (2017) 35-49.

- [26] H.T. Thai, D.H. Choi, A simple first-order shear deformation theory for the bending and free vibration analysis of functionally graded plates, *Compos. Struct.*, 101 (2013) 332-340.
- [27] K. Khorshidi, A. Fallah, Buckling analysis of functionally graded rectangular nano-plate based on nonlocal exponential shear deformation theory, *Int. J. Mech. Sci.*, 113 (2016) 94-104.
- [28] K. Khorshidi, A. Fallah, Effect of exponential stress resultant on buckling response of functionally graded rectangular plates, *J. Stress Anal.*, 2(1) (2017) 27-33.
- [29] P. Shi, C. Dong, F. Sun, W. Liu, Q. Hu, A new higher order shear deformation theory for static, vibration and buckling responses of laminated plates with the isogeometric analysis, *Compos. Struct.*, 204 (2018) 342-358.
- [30] H. Tanzadeh, H. Amoushahi, Buckling and free vibration analysis of piezoelectric laminated composite plates using various plate deformation theories, *European J. Mech. Solids*, 74 (2019) 242-256.
- [31] P.L. Pasternak, On a New Method of an Elastic Foundation by Means of Two Foundation Constants, *Gosudarstvennoe Izdatelstvo Literaturi po Stroitelstvu Arkhitekture*, (1954).
- [32] A. Kutlu, M.H. Omurtag, Large deflection bending analysis of elliptic plates on orthotropic elastic foundation with mixed finite element method, *Int. J. Mech. Sci.*, 65(1) (2012) 64-74.
- [33] A.S. Sayyad, Y.M. Ghugal, Bending and free vibration analysis of thick isotropic plates by using exponential shear deformation theory, *Appl. Comput. Mech.*, 6(1) (2012) 65-82.
- [34] Y.M. Ghugal, A.S. Sayyad, Free vibration of thick orthotropic plates using trigonometric shear deformation theory, *Lat. Am. J. Solids Struct.*, 8(3) (2011) 229-243.
- [35] M. Karama, K.S. Afaq, S. Mistou, A new theory for laminated composite plates, *Proceedings of the Institution of Mechanical Engineers, Part L: J. Mater. Des. Appl.*, 223(2) (2009) 53-62.
- [36] E. Reissner, On transverse bending of plates, Including the effect of transverse shear deformation, *Int. J. Solids Struct.*, 11(5)(1974) 567-573.
- [37] L.L. Ke, C. Liu, Y.S. Wang, Free vibration of nonlocal piezoelectric nanoplates under various boundary conditions, *Physica E*, 66 (2015) 93-106.
- [38] K. Khorshidi, M. Karimi, Analytical modeling for vibrating piezoelectric nanoplates in interaction with inviscid fluid using various modified plate theories, *Ocean Eng.*, 181 (2019) 267-280.
- [39] M. Bahreman, H. Darijani, A.B. Fard, The size-dependent analysis of microplates via a newly developed shear deformation theory, *Acta Mech.*, 230(1) (2019) 49-65.